Proposal of Reduced Parts Slotless Planar Resolver

F. Zare*, and F. Tootoonchian** (C.A.)

Abstract: The Recent development of 2-DOF electrical machines leads to increasing need for 2-DOF position sensors. Using a planar sensor instead of two linear ones decreases the complexity, and cost of the employed drive. Therefore, in this paper a new slotless configuration is proposed for the planar resolver, that simplifies the manufacturing of the sensor. Then, the optimal combination of the stator/mover number of coils is determined based on the proposed analytical model. Finally, to reduce the number of integrated parts of the proposed resolver, a new configuration with skewed coils is proposed. The success of the developed model and the presented configuration is validated using three-dimensional finite element analysis.

1 Introduction

LINEAR machines are increasingly using in different industrial applications. Their closed-loop control system needs the information of mover position. Although sensorless position estimation has many advocates, in high performance control systems still position sensors have their advantages. Commercial linear position sensors are LVDTs, linear encoders and linear resolvers [1]-[3]. LVDTs benefit from accurate position determination, low cost and easy installation. However, their measuring range is limited to 50 cm [4]. The next, linear encoders, have wider measuring range. But, their accuracy is affected in harsh and noisy environments where there is wide temperature variation, high vibration, noise and pollution [5]. In such applications, linear resolvers are the best choice.

Linear resolvers are divided in two main groups: Wound Mover (WM) resolvers and Variable Reluctance (VR) ones. In WM resolvers, both the mover and the stator have windings. The mover includes the excitation coils and the stator includes the sine and the cosine coils [4]. While, in VR resolvers all the coils are located on one part and the next is a solid ferromagnetic core with a special shape to satisfy the VR function. Since the reluctance of the ferromagnetic core is much less than that of the air-gap region, the variation of the reluctance in VR resolvers is defined based on the variation of air-gap reluctance. Therefore, two types of VR resolvers are proposed based on variable air-gap length [6] and variable area [7].

The design criteria of the linear WM resolvers are discussed in [4]. Then, the influence of winding's pole number on the sensor's position error is considered in [8]. The presentation of different mechanical faults for linear sensors is defined in [9]. Since the design and optimization is iterative process, developing an analytical model with high precision and low calculating burden is always interesting subject. Therefore, in [10] a layer model is developed for the linear WM resolver. Although the proposed model of [10] could consider the influence of different winding arrangements, slot-tooth region and the windings' pole number, longitudinal end effect as the most important phenomena in performance of linear sensors is not involved in the model. To consider the effect of cores' limited length in the model, a subdomain model is presented in [11]. The results of the subdomain model of [11] are perfectly verified by experimental measurements and finite element analysis. However, the computational burden of the proposed method was comparable with the Finite Element Method

(FEM). Therefore, the same authors, proposed some simplifications in [12] to reduce the calculation time without accuracy deterioration.

Linear VR resolvers are also considered in many researches. Accuracy improvement of them is studied in [13]-[14] and their analytical modeling based on Magnetic Equivalent Circuit (MEC) model is investigated in [15]-[17]. Winding function method is used for performance evaluation of VR resolvers in [18]-[19].

All the mentioned researches are done on 1-DOF linear resolvers. Planar resolvers that are used to detect position in a plane are presented in [20]-[21] for the first time. The design aspects of them are studied using FEM and a sample of the sensor is constructed and tested in [20]. The challenges of using two sensors instead of a planar one is discussed in [21]. Then, an analytical model based on MEC method is proposed for it in [22]. The studied design of [20]-[22] has slotted configuration with a specific stator-mover slot numbers. However, in this paper a slotless structure is presented for the planar resolver. Using the slotless configuration gives higher degree of freedom to the designer for winding configuration and also significantly simplifies the manufacturing process of the sensor. Also, a mathematical winding function model is developed for performance evaluation of the proposed slotless planar resolver. The results of the model are verified by comparing them with those of 3-D finite element method. Then, the optimal number of stator/mover number of coils are determined to achieve the highest accuracy. Finally, to reduce the number of parts using skewed coils is proposed for the developed planar resolver.

2 Initial Design

The optimal configuration of [20] with removing slot-tooth region is considered as the initial design of current study. Fig. 1 shows the mover of the proposed resolver. Two perpendicular excitation winding is considered for the x- and y-axis movement. Sinusoidal distribution with variable turn coils, as given in Fig. 2, is considered for the excitation windings.

As it can be seen in Fig. 3, the same as mover, the stator has orthogonal windings in x- and y-direction that can detect position in each direction. Table. I shows the physical dimensions of proposed resolver. Fig. 4 denotes the winding arrangement of signal windings.

3 Proposed Mathematical Model

The proposed mathematical model for characteristic investigation of the planar resolver is winding function method. In this method the inductances of the sensor are
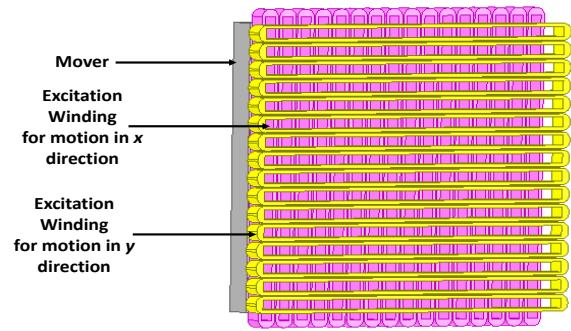

Fig. 1 The Mover ferromagnetic core and excitation windings
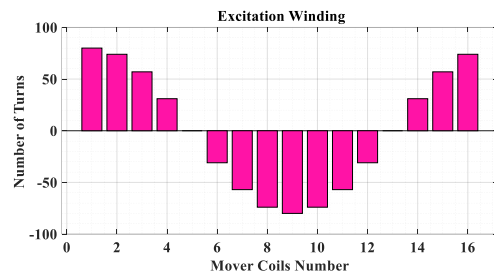
Fig. 2 The turn number of the mover's coils

calculated based on windings' turn function. Since there is no slot-tooth region and the flux density in the back iron is in the linear part of the magnetization curve of the core material, the performance of the studied resolver is only influenced by the windings' distribution. On the other hand, the winding function method precisely consider the windings configuration. Therefore, is can be
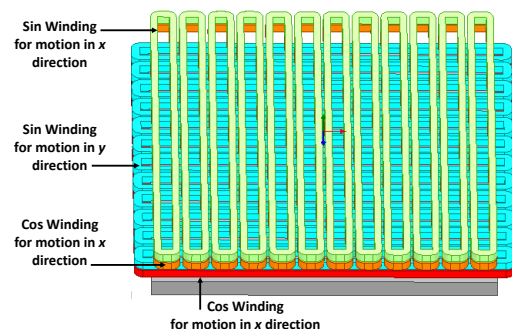

Fig. 3 The sine and the cosine windings of the developed resolver

Table. 1 Physical dimensions of proposed resolver

|	
Stator length/ width	40 mm./ 40 mm.
Mover length/ width	80 mm./ 80 mm.
Stator height	4mm
Mover height	4mm.
Number of x / y excitation coils	16 / 16
Number of x / y signal coils	12 / 12
The signal windings' arrangement	Overlapping, variable turn coils
The excitation winding arrangement	Single-phase variable turn
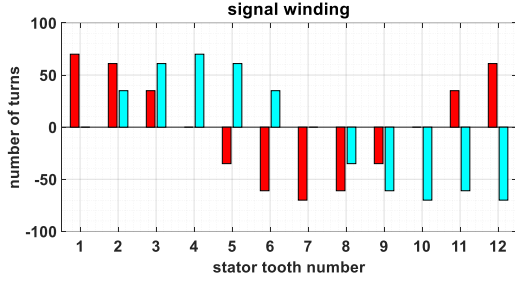
Fig. 4 The number of turns on each stator's tooth, red: cosine coils, and turquoise: sine coils
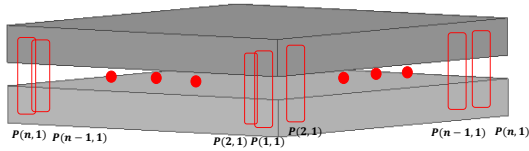

Fig. 5 Ampere's law path in proposed resolver

a good choice for determining the output characteristic of the developed resolver.

The implementation of the mathematical method is started by the Ampere's law:

$$\oint H.\,dl = n(x/y).\,i \tag{1}$$

where H denotes the magnetic field vector. $n(x/y)$ and i are the turn number and the excitation current, respectively. Considering the arbitrary closed paths of Fig. 5, Eq. (1) can be re-written as:

$$\oint_{Pn} H.\,dl = n_n(x)i_n(x) + n_n(y)i_n(y) \tag{2}$$

$$\sum_{q=1}^{n_s} \oint_{p(x,y)} H_q.\,dl_q = \sum_{q=1}^{n_s} n_{nq}(x)i_{nq}(x) + n_{nq}(y)i_{nq}(y) \tag{3}$$

Since the coils are connected in series, they carry the equal current. Therefore, (3) can be written as:

$$\sum_{q=1}^{n_s}\sum_{q=1}^{n_s} \oint_{P(x,y)} H_q.\,dl_q$$
$$= i(x) \sum_{q=1}^{n_s} n_{nq}(x) \tag{4}$$
$$+ i(y) \sum_{q=1}^{n_s} n_{nq}(y)$$

Considering the desired path of Fig. 6, the left-hand side of (4) can be written as:

$$\oint_{P(x,y)} H.\,dl = H_{12}.\,l_{12} + H_{23}.\,l_{23} + H_{34}.\,l_{34}$$
$$+ H_{45}.\,l_{45} + H_{56}.\,l_{56} \tag{5}$$
$$+ H_{67}.\,l_{67} + H_{78}.\,l_{78}$$
$$+ H_{81}.\,l_{81}$$

Assuming infinite relative permeability for the ferromagnetic back-iron, (5) is simplified to:

$$\oint_{P(x,y)} H.\,dl = H_{34}.\,l_{34} + H_{78}.\,l_{78} \tag{6}$$

Substituting (6) into (4):

$$\sum_{q=1}^{n_s}\sum_{q=1}^{n_s} H_{34}.\,l_{34} + H_{78}.\,l_{78}$$
$$= i(x) \sum_{q=1}^{n_s} n_{nq}(x) \tag{7}$$
$$+ i(y) \sum_{q=1}^{n_s} n_{nq}(y)$$

Considering the motion in x-direction, as shown in Fig.7, the summation of winding's turn in y-direction is equal to zero. Therefore:

$$\sum_{q=1}^{n_s} H_{34}.\,l_{34} + H_{78}.\,l_{78} = i(y) \sum_{q=1}^{n_s} n_{nq}(y) \tag{8}$$

In Fig.7 for each desired x:

$$H(x,y) = H(x, y+1) \tag{9}$$

Therefore, (7) can be written as:

$$H(y) = i(y) \sum_{q=1}^{n_s} n_{nq}(y) \tag{10}$$


Fig. 6 Ampere's law path
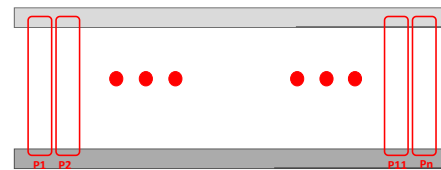
Fig. 7 2-DoF resolver in x direction

It means the studied planar resolver has the independent performance for each direction. So, the problem can be solved for linear wound rotor resolver as below:

$$\int_{12561}^{\square} H.\,dl = \int_S^{\square} \vec{J}.\overrightarrow{ds} \tag{11}$$

Therefore:

$$F_{12} + F_{25} + F_{56} + F_{61} = n(y,y')i \tag{12}$$

F_{12} and F_{56} can be assume as zero. and

$$\int_0^L \int_0^l \mu_0 H(y,y')dz\,dx = 0 \tag{13}$$

Where L is the length of mover. Therefore:

$$\int_0^L \frac{\mathcal{F}(y,y')}{l_g}dy = 0 \tag{14}$$

where l_g is equivalent air gap length and is constant in the length of mover and is equal to the distance between stator and mover.

$$\int_0^L \frac{\mathcal{F}_{da}(0,y') + \mathcal{F}_{bc}(y,y')}{l_g(y,y')}dy = \int_0^L \frac{n(y,y')}{l_g(y,y')}i\,dy = 0 \tag{15}$$

where:

$$\mathcal{F}_{da}(0,y') = \frac{1}{L \times < l_g^{-1}(y,y') >}\int_0^L \frac{n(y,y')}{l_g(y,y')}i\,dy \tag{16}$$

where $< l_g^{-1}(y,y') >$ is the average of reverse of the air gap function. Therefore:

$$\mathcal{F}_{bc}(y,y') = i\,n(y,y') - \frac{i}{L \times < g^{-1}(y,y') >}\int_0^L \frac{n(y,y')}{l_g(y,y')}i\,dy \tag{17}$$

where:

$$N(y,y') = n(y,y') - < n(y,y') > \tag{20}$$

$$M(y,y') = n(y,y') - < M(y,y') > \tag{21}$$

$$< n(y,y') > = \frac{1}{L}\int_0^L n(y,y')dy \tag{22}$$

$$< M(y,y') > = \frac{1}{L \times < l_g^{-1}(y,y') >} \times \int_0^L n(y,y')dy \tag{23}$$

The magneto motive force of the air-gap due to the mover current, I_{exc}, is:

$$\mathcal{F}_{exc} = M_{exc}(y,y') \times I_{exc} \tag{24}$$

Also, the differential air-gap flux is:

$$d\varphi = \mathcal{F}_{exc}(y,y')\mu_0 l l_g^{-1}(y,y')dy \tag{25}$$

Then, the flux linkage of the kth coil of the signal windings can be determined as:

$$\varphi_{k-k'} = \int_0^L n_{s,c-k}(y,y').\mathcal{F}_{exc}(y,y')g^{-1}(y,y')dy \tag{26}$$

Finally, total flux linkage of the stator windings is:

$$\lambda_{exc-s,c} = \sum_{k=1}^q \varphi_{k-k'} = \mu_0 l(\sum_{k=1}^q \int_0^L n_{s,c-k}(y,y').\mathcal{F}_{exc}(y,y') \times l_g^{-1}(y,y')dy) \tag{27}$$

Afterwards, the mutual inductance between the excitation and signal windings is obtained as:

$$L_{exc-s,c} = \mu_0 l \int_0^L n_{s,c}(y,y').M_{exc}(y,y') \times l_g^{-1}(y,y')dy \tag{28}$$

where:

$$M_{exc} = \mu_0 l \int_0^L n_{exc}(y,y').M_{exc}(y,y') \times g^{-1}(y,y')dy \tag{29}$$

Then, the induced voltages in the signal winding can be determined as:

$$v_{sin} = \frac{d\lambda_{exc-s}}{dt} = \frac{d}{dt}(L_{exc-s}I_{exc}) \tag{31}$$

$$v_{cos} = \frac{d\lambda_{exc-c}}{dt} = \frac{d}{dt}(L_{exc-c}I_{exc}) \tag{32}$$

And assuming the excitation voltage equal to $v_m \cos(\omega t)$, and the resistance and inductance of the excitation winding equal to R_{exc}, and L_{exc}, the excitation current is calculated as:

$$I_{exc} = \frac{v_m}{\sqrt{R_{exc}^2 + L_{exc}^2 \omega^2}}\cos(\omega t - tan^{-1}\frac{L_{exc}\omega}{R_{exc}}) \tag{30}$$

4 Model Verification

Time Stepping Finite Element Analysis (TSFEA) is

the most accurate simulation method for electromagnetic

Parameter	WFM	3-D-TSFEM
Voltage amplitude (V)	1.078	1.082
AAPE(mm)	0.007	0.007
MPE(mm)	0.018	0.016
Excitation winding self-inductance (mH)	7.52	7.53
Sin-Exc inductance amplitude (mH)	4.72	4.87
Cos-Exc inductance amplitude (mH)	4.73	5.20
Simulation Time	30 sec	139 h

sensors. Therefore, to verify the success of the developed model its results are compared with those of 3-D TSFEA obtained by Ansysis Electronics Desktop 2020 R2.

Before calculating the induced voltages, the inductances of the windings are determined. It is expected to have a constant value for the self-inductance of the mover coils. As it can be seen in Fig. 8, the calculated inductance has an almost constant value. Also, the predicted value using the proposed model is 7.52 mH and that of TSFEA is 7.53 mH. It means there is 0.1% deviation between the results.

Fig. 9 shows the mutual inductance between the stator's sine and cosine windings and the mover's winding. As expected, the inductances have sinusoidal variation with 90 ° phase difference. The maximum deviation of the predicted value for the mutual inductances with the calculated value of the TSFEA is 9.09%.

The output voltages, calculated using winding function method in x- and y-direction signal windings are shown in Figs. 10-a, and –b, respectively. Those voltages calculated using the TSFEA, are given in Figs. 11-a, and
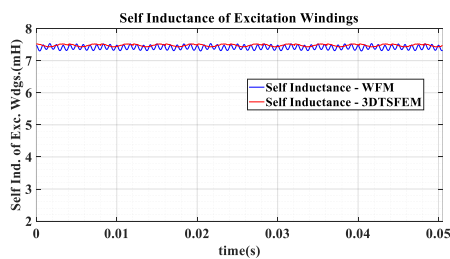

Fig. 8 Self-inductance of the mover winding
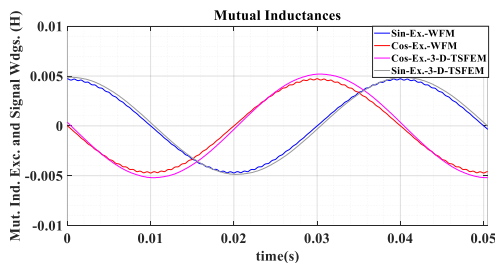
Fig. 9 Mutual inductances between the signal windings with the excitation winding

–b, respectively. It should be noted that the velocity in x- and y- direction can be set completely independent.

The envelope of the amplitude modulated voltages is determined based on the peak detection method. Then, the inverse tangent of the envelope's ratio is used to calculate the mover position as given in Fig. 12. The calculated position is compared with the reference position to determine the position error of the sensor. The AAPE of the sensor for each direction calculated by TSFEA and the developed model is 7 μm and the MPE calculated by winding function model and the TSFEA is 18 μm, and 16 μm, respectively. Close agreement between the results of the developed model and the TSFEA, confirms the success of the proposed model. The simulation time of the proposed model is 30 seconds, while that time for the TSFEA is 144 hours. Therefore, the presented model is very fast and yet precise. The results of the winding function method are compared with those of TSFEA in Table II.

5 The Combination of Stator/Mover Number of Coils

The FEM is the most precise method to investigate the output of proposed resolver but due to its high computational burden, it cannot be used for optimization purpose. Hence, to optimize the number of coils in excitation and signal windings, the proposed winding function method (WFM) is employed. The different combination of excitation and signal windings are considered and the MPE and AAPE are calculated for each combination, as presented in Figs.13-a, and –b, respectively. An interesting application of Fig. 13 is


(a)

(b)
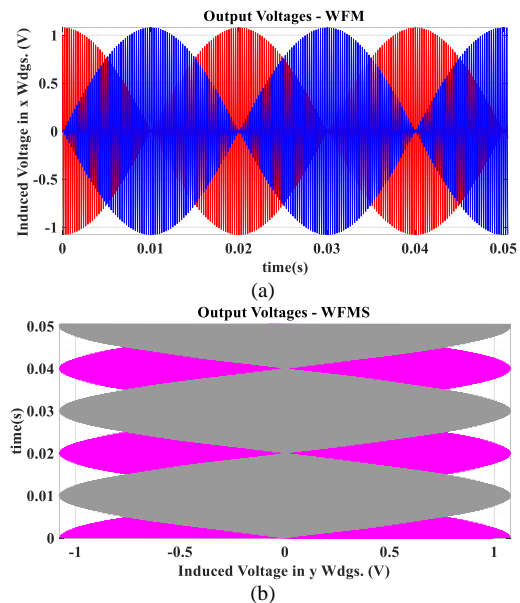
Fig. 10 The induced voltages in the signal windings of planar resolver, calculated by winding function model: (a) x-direction windings, and b) y-direction windings.
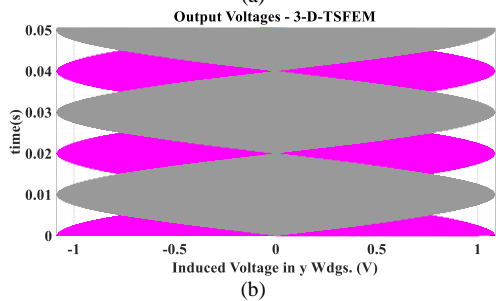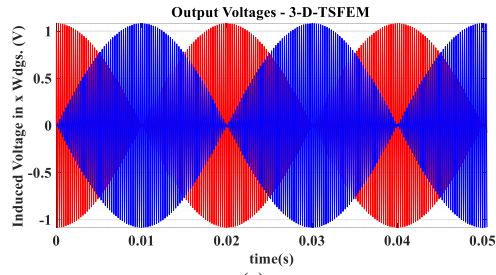
Fig. 11 The induced voltages in the signal windings of planar resolver, calculated by 3-D TSFEA: (a) x-direction windings, and b) y-direction windings.
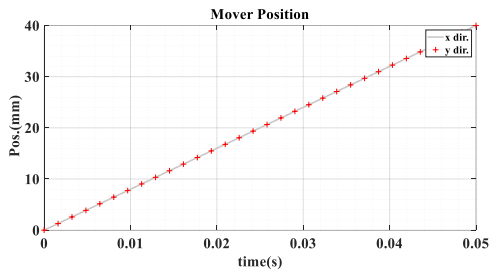

**Fig. 12** The calculated position of the mover
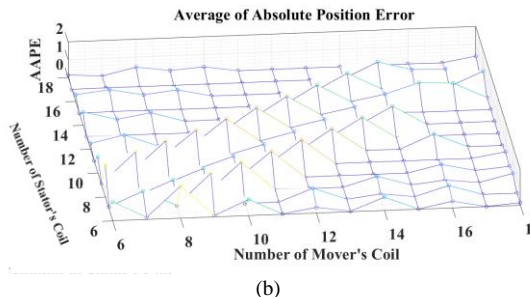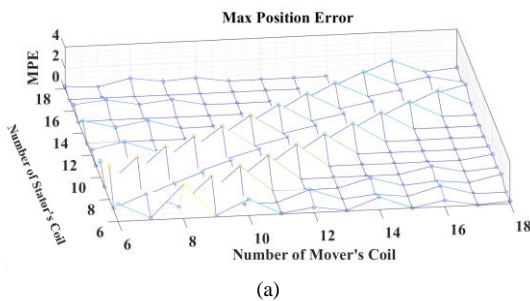
**Fig. 13** The combinations of the mover/stator number of coils on sensor's accuracy: (a) MPE, and (b)AAPE
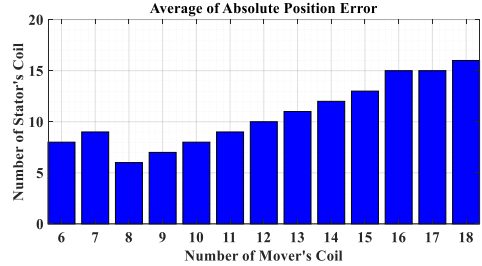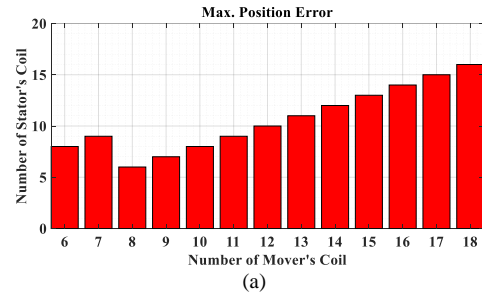
Fig. 14 The number of signal coil's that maximize the position error for a specific number of mover coils: (a) MPE, and (b) AAPE
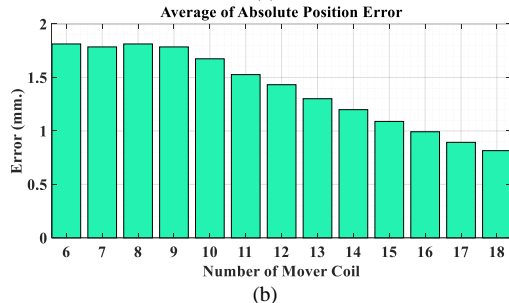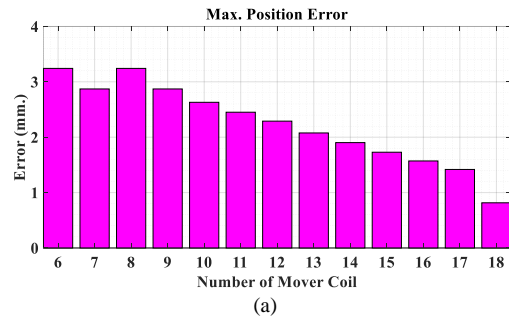

Fig. 15 The worst value of the position error for the given number of mover coils: (a) MPE, and (b) AAPE

determining the bad combinations that lead to higher position error of the sensor. For example, for a specific number of the mover coils, the number of stator coils that leads to the worst MPE is given in Fig. 14-a, and its number for the highest AAPE is shown in Fig. 14-b. The relevant position errors are shown in Fig. 15.

On the other side, the number of stator coils to achieve the minimum MPE and AAPE with a given number of mover coils are given in Figs. 16-a, and –b, respectively. The relevant position errors are shown in Fig. 17. From Fig. 17-a, the best accuracy of the studied planar resolver is achieved when the combination of 14 mover
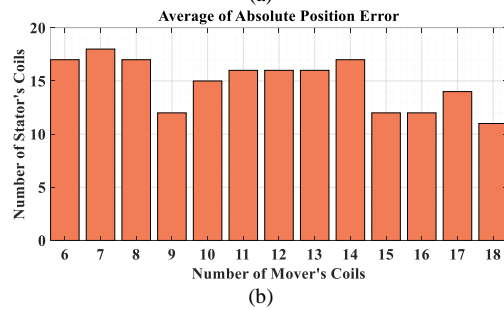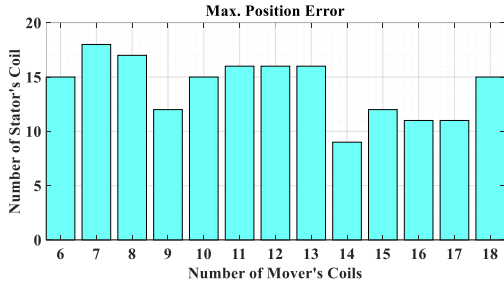
Fig. 16 The number of signal coil's that minimize the position error for a specific number of mover coils: (a) MPE, and (b) AAPE
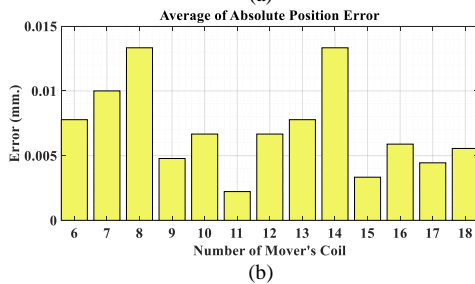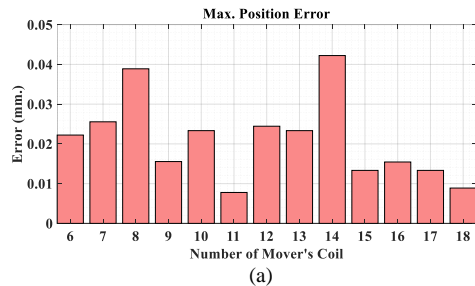

Fig. 17 The worst value of the position error for the given number of mover coils: (a) MPE, and (b) AAPE

mover coils with 9 stator coils is used. The AAPE of the optimal sensor is 2.2 μm while that value for the initial design was 7 μm. It means using the combination of 11-9 coils for mover-stator in comparison with the combination of 16-12 has 68.5% higher accuracy.

6 Using skewed coils

The developed resolver can detect position in both x and y direction. But employing two excitation windings and two signal windings, makes it complicated. So, a new flat configuration that can be able to detect position in both x and y direction with more simple construction

is needed.

Suppose A as a desirable point on the x- excitation winding. If A rotates around y-axis, the x-direction resolver will work correctly because it seems the x-excitation winding is skewed versus x-signal windings, as shown in Fig. 18-a. Skewing excitation winding is a common method for accuracy improvement in rotational resolvers and here the same technique is used for the planar resolver. Using the same skewed excitation winding, the induced voltages in the y-axis signal windings are also amplitude modulated signals. Therefore, the induced voltage in y-axis windings can be used for determining the y-position. In fact, if the skewing angle of the new excitation winding with the x-axis signal winding is equal to θ, then the relevant angle with the y-axis signal windings will be equal to $\frac{\pi}{2} - \theta$, as shown in Fig. 18-b.

Therefore, the proposed planar resolver can work correctly using a single excitation winding which is skewed with respect to the signal windings.

Considering the motion along x-axis, the induced voltages in the x-signal windings are given in Fig.19. As it can be seen the induced voltages are amplitude modulated. It means the proposed configuration works correctly to determine the position. However, the calculated position error of the sensor, as shown in Fig. 20, is higher than the initial designed one. It means simplifying the practical implementation is achieved in the price of accuracy reduction. The MPE and the AAPE of the reduced parts sensor is equal to 19 μm and 8 μm respectively. While those values for the primary design were 16 μm and 7 μm, respectively.
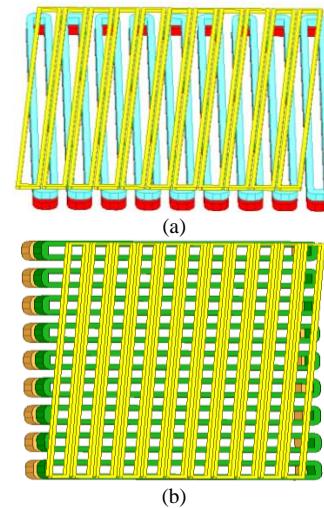

Fig. 18 Using a skewed excitation winding for planar resolver (the back-iron is removed to clearly show the windings: (a) skewed excitation winding and the non-skewed x-signal windings, and (b) skewed excitation winding and the non-skewed y-signal windings
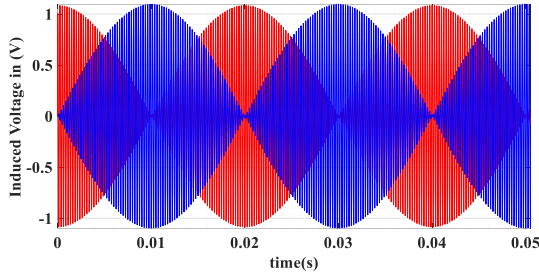
Fig. 19 The output voltage of x-signal windings using the skewed excitation winding.
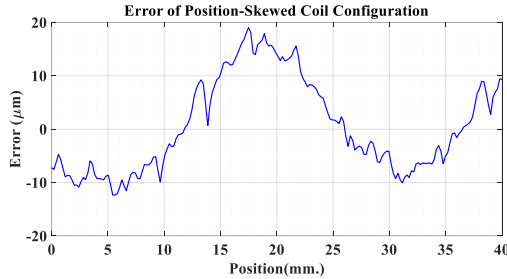

Fig. 20 The position error of the reduced parts planar resolver

The detailed sizes of equations are Full: 10pt, Subcript/Superscript: 5pt, Sub- Subcript/Superscript: 4pt, Symbol: 13pt and Sub-Symbol: 10pt and equations are non-italic and non-bold.

$$K^{-1} = F_u \left(\begin{bmatrix} -0.1 & M^{-1} \\ -0.1 & M^{-1} \end{bmatrix}, \delta_m \right) \tag{1}$$

Be sure that the symbols in your equation have been defined before the equation appears or immediately following. When you refer to equations in the text, refer to "Eq. (1)" or "Equation (1)" except at the beginning of a sentence: "Equation (1) is used"

7 Conclusion

In this paper a 2DoF planar resolver was presented. The developed resolver had slotless configuration with perpendicular windings. Eliminating the slot-tooth region of the core, significantly simplified the manufacturing process of the sensor in comparison with the previously developed slotted planar sensors. The winding function model was proposed to evaluate the performance of the sensor and the its accuracy was confirmed by 3-D-TSFEM. Then, the developed model was empolyed to determine the optimal combination of the stator and mover coils' number. Finally, a reduced parts sensor with only one skewed excitation winding was proposed and it was shown that such a configuration could reduce the copper usage of sensor in the price of slightly higher position error.

References

[1] P. Naderi, A. Ramezannezhad and L. Vandevelde, "A Novel Linear Resolver Proposal and Its Performance Analysis Under Healthy and Asymmetry Air-Gap Fault," in *IEEE Transactions on Instrumentation and Measurement*, vol. 71, pp. 1-9, 2022, Art no. 9504109, doi: 10.1109/TIM.2022.3155747.

[2] P. Naderi, R. Ghandehari and M. Heidary, "A Comprehensive Analysis on the Healthy and Faulty Two Types VR-Resolvers with Eccentricity and Inter-Turn Faults," in *IEEE Transactions on Energy Conversion*, vol. 36, no. 4, pp. 3502-3511, Dec. 2021, doi: 10.1109/TEC.2021.3079725.

[3] P. Naderi and R. Ghandehari, "Comprehensive Analysis on a New Type VR-Resolver with Toroidal Windings Under Healthy and Eccentric Cases," in *IEEE Transactions on Industrial Electronics*, vol. 69, no. 12, pp. 13754-13762, Dec. 2022, doi: 10.1109/TIE.2021.3130318.

[4] Z. Nasiri-Gheidari, "Design, Performance Analysis, and Prototyping of Linear Resolvers," in *IEEE Transactions on Energy Conversion*, vol. 32, no. 4, pp. 1376-1385, Dec. 2017, doi: 10.1109/TEC.2017.2718555.

[5] Alipour-Sarabi, "Use of Resolvers in Limited Rotations," in *IEEE Transactions on Energy Conversion*, vol. 37, no. 3, pp. 2019-2026, Sept. 2022, doi: 10.1109/TEC.2022.3144182.

[6] A. Daniar and Z. Nasiri-Gheidari, "The influence of different configurations on position error of linear variable reluctance resolvers," 2017 Iranian Conference on Electrical Engineering (ICEE), 2017, pp. 955-960, doi: 10.1109/IranianCEE.2017.7985177.

[7] M. Bahari and Z. Nasiri-Gheidari, "Longitudinal End Effect in a Variable Area Linear Resolver and its Compensating Methods," in Iranian Conference on Electrical Engineering (ICEE), Mashhad, Iran, 2018.

[8] H. Saneie, Z. Nasiri-Gheidari and F. Tootoonchian, "The influence of winding's pole pairs on position error of linear resolvers," *2017 Iranian Conference on Electrical Engineering (ICEE)*, Tehran, Iran, 2017, pp. 949-954, doi: 10.1109/IranianCEE.2017.7985176.

[9] A Daniar, Z Nasiri-Gheidari, F Tootoonchian, "Position Error Calculation of Linear Resolver under Mechanical Fault Conditions", *IET Science, Measurement & Technology*, vol. 11, no. 7, pp. 948 - 954, 2017

[10] H Saneie, Z Nasiri-Gheidari, and F Tootoonchian, "Analytical model for performance prediction of linear resolver", *IET Electric Power Applications*, vol. 11, no. 8, pp. 1457-1465, 2017

[11] A. Paymozd, H. Saneie, Z. Nasiri-Gheidari and F. Tootoonchian, "Subdomain Model for Predicting the Performance of Linear Resolver Considering End Effect and Slotting Effect," in *IEEE Sensors Journal*, vol. 20, no. 24, pp. 14747-14755, 15 Dec.15, 2020, doi: 10.1109/JSEN.2020.3010785.

[12] A. Paymozd, H. Saneie, A. Daniar and Z. Nasiri-Gheidari, "Accurate and Fast Subdomain Model for Electromagnetic Design Purpose of Wound-Field Linear Resolver," in *IEEE Transactions on Instrumentation and Measurement*, vol. 70, pp. 1-8, 2021, Art no. 9003408, doi: 10.1109/TIM.2021.3080400.

[13] A. Keyvannia and Z. Nasiri-Gheidari, "A Comprehensive Winding Method for Linear Variable-Reluctance Resolvers to Compensate for the End Effects," in *IEEE Transactions on Industrial Electronics*, vol. 70, no. 9, pp.

9593-9600, Sept. 2023, doi: 10.1109/TIE.2022.3210572.

[14] A. Ramezannezhad, P. Naderi and L. Vandevelde, "A Linear Position Sensor Proposal by Development of a Variable Reluctance Linear Resolver," *2022 30th International Conference on Electrical Engineering (ICEE)*, Tehran, Iran, Islamic Republic of, 2022, pp. 570-576, doi: 10.1109/ICEE55646.2022.9827303.

[15] S. A. Seyed-Bouzari, H. Saneie and Z. Nasiri-Gheidari, "Analysis and Compensation of the Longitudinal End-Effect in Variable Reluctance Linear Resolvers Using Magnetic Equivalent Circuit Model," in *IEEE Transactions on Transportation Electrification*, doi: 10.1109/TTE.2023.3239500.

[16] P. Naderi, A. Ramezannezhad and L. Vandevelde, "Performance Analysis of Variable Reluctance Linear Resolver by Parametric Magnetic Equivalent Circuit in Healthy and Faulty Cases," in *IEEE Sensors Journal*, vol. 21, no. 18, pp. 19912-19921, 15 Sept.15, 2021, doi: 10.1109/JSEN.2021.3094798.

[17] A. Ramezannezhad, P. Naderi and L. Vandevelde, "A Novel Method for Accuracy Improvement of Variable Reluctance Linear Resolvers," in *IEEE Sensors Journal*, vol. 22, no. 19, pp. 18409-18417, 1 Oct.1, 2022, doi: 10.1109/JSEN.2022.3199807.

[18] A. Daniar, Z. Nasiri-Gheidari and F. Tootoonchian, "Performance Analysis of Linear Variable Reluctance Resolvers Based on an Improved Winding Function Approach," *IEEE Transactions on Energy Conversion*, vol. 33, no. 3, pp. 1422-1430, 2018.

[19] M. Bahari, R. Alipour-Sarabi, Z. Nasiri-Gheidari and F. Tootoonchian, "Proposal of Winding Function Model for Geometrical Optimization of Linear Sinusoidal Area Resolvers," in *IEEE Sensors Journal*, vol. 19, no. 14, pp. 5506-5513, 15 July15, 2019, doi: 10.1109/JSEN.2019.2908926.

[20] R. Faryadras and F. Tootoonchian, "Design and Experimental Investigation of a Two-DOF Planar Resolver," in *IEEE Transactions on Instrumentation and Measurement*, vol. 71, pp. 1-8, 2022, Art no. 9000408, doi: 10.1109/TIM.2021.3139656.

[21] R. Faryadras, and F. Tootoonchian, "The Proposal of a 2-DOF Resolver for Linear Motion", *Scientific Journal of Applied Electromagnetics*, vol. 10, no. 1, pp. 81-90, 2022

[22] F. Zare, F. Tootoonchian, A. Daniar, M. C. Gardner and B. Akin, "Magnetic Equivalent Circuit Model for Performance Prediction of Two-DOF Planar Resolver," in *IEEE Access*, vol. 11, pp. 102207-102216, 2023, doi: 10.1109/ACCESS.2023.3315344.

Fateme Zare received the B.Sc. degree in electrical engineering from the Sharif University of Technology, Tehran, Iran, in 2016, the M.Sc. degree in electrical engineering from Isfahan University of Technology, Isfahan, Iran, in 2018, and the Ph.D. degree in electrical engineering from the Sharif University of Technology, Tehran, Iran, in 2022. She is currently an Assistant Professor with the Department of Electrical and Computer Engineering, Isfahan University of Technology. Her research interests include design and optimization of electrical machines and electromagnetic sensors.

Farid Tootoonchian received the B.Sc. and M.Sc. degrees in electrical engineering from the Iran University of Science and Technology, Tehran, Iran, in 2000 and 2007, respectively, and the Ph.D. degree from the K. N. Toosi University of Technology, Tehran, in 2012. He is currently an Associate Professor with the Department of Electrical Engineering, Iran University of Science and Technology. His research interests include design, optimization, finite-element analysis, and prototyping of ultrahigh-speed electrical machines and ultrahigh-precision electromagnetic sensors.